JOURNAL OF APPLIED ELECTROCHEMISTRY 21 (1991) 829–836

Passivity of α-brass (Cu : Zn/67 : 33) and its breakdown in neutral and alkaline solutions containing halide ions

A. G. GAD-ALLAH, M. M. ABOU-ROMIA, M. W. BADAWY, H. H. REHAN

Department of Chemistry, Faculty of Science, Cairo University, Giza, Egypt

Received 24 April 1990; revised 15 January 1991

The passivation behaviour of α-brass (Cu : Zn = 67 : 33) in alkaline solutions was studied using cyclic voltammetry and potentiostatic current transient measurements. The recorded cyclic voltammograms exhibited the main features usually observed for pure copper and zinc, and one additional anodic peak on the reverse potential scan. The height, sharpness and location of the different peaks depended greatly on the alkali concentration and the scan rate. The results show that the formation of Cu_2O and $Cu(OH)_2$ films proceed under ohmic resistance control following a dissolution-precipitation mechanism. The effect of F^-, Cl^- and Br^- ions on the passivity was also studied. The pitting potential was found to decrease with logarithm of halide ion concentration. The current transients in the absence and presence of halide ions were analysed. In the absence of pitting the current, after a few seconds, was found to increase linearly with the reciprocal of the square root of time while in the presence of pitting it was found to fit the Engell-Stolica equation.

1. Introduction

The anodic dissolution of Cu/Zn alloys in neutral and alkaline solutions has been studied with special attention to dezincification [1–16]. The stress cracking of many brasses and the role of dezincification has been widely investigated [17–24]. The electrochemical behaviour of some Cu/Zn alloys in NaOH solutions upon alternate anodic and cathodic galvanostatic polarization was studied by Shams El-Din and Abd El-Wahab [1]. The anodic behaviour of Cu/Zn alloys with 15.9, 46.8 and 50.5 wt % Zn was found to resemble that of pure Cu showing oxidation arrests, corresponding to the formation of Cu_2O, $Cu(OH)_2$ and Cu_2O_3 before O_2-evolution. Generally, the preferential dissolution of Zn from Cu/Zn alloys occurs more predominantly with Zn rich than with Cu rich alloys [3, 5, 11]. A wide range of techniques [4, 9–11, 19] has been used to distinguish between dezincification by a selective dissolution mechanism as compared to an ionization redeposition mechanism.

In the present study, the cyclic voltammetry and the potentiostatic current transients of α-brass (67% Cu, 33% Zn) in alkaline solutions were investigated. The effect of halide ions was also studied.

2. Experimental details

The disc electrodes used were cut from commercial grade annealed α-brass (Helwan Co. of Non-Ferrous Industries, Egypt) of composition Cu : 67.28, Pb : 0.029, Fe : 0.002 and Zn : 32.26. The specimens were annealed at 600° C for 1 h and air-cooled. The electrode area was 0.30 cm^2. The electrode preparation, the electrolytic cell, the potentiodynamic circuit and other experimental details were essentially the same given elsewhere [25, 26]. All solutions were prepared from AnalaR grade chemicals and triply distilled water. The alkaline solutions used were 1.0, 0.5, 0.25, 0.10, 0.05 and 0.01 M NaOH and borate buffer solutions of pH 7.26 (0.005 M borate + 0.18 M H_3BO_3), 9.24 (0.075 M borate + 0.015 M H_2BO_3) and 10.18 (0.024 M borate + 0.042 M NaOH). All potentials were measured and referred to the saturated calomel electrode (SCE). The experiments were conducted at 30 ± 0.2° C.

In cyclic voltammetry experiments, the electrode was left at −1.00 V for 3 min before starting the potential scan to more anodic values. Potentiostatic current transients were recorded after stepping the potential from the steady open circuit value to a preset E_s value.

3. Results and discussion

3.1. *Cyclic voltammetry*

The main features of the cyclic voltammograms (CVs) recorded for α-brass in alkaline solutions depend greatly on the alkali concentration, scan rate and the potential range over which the CVS were recorded, as can be seen in Figs 1 and 2. Generally, the peak resolution and height increase with alkali concentration. The potential scan in the anodic direction was always started at a present potential, E_s = −1.00 V which is more anodic to the peaks corresponding to the oxidation of Zn [27, 28]. Thus the electrode surface is assumed to be covered with $Zn(OH)_2$ layer before the potential scan. Comparing the anodic peaks recorded at potentials > −1.00 V for α-brass

0021-891X/91 $03.00 + .12

Table 1. The peak currents and potentials for α-brass in NaOH solutions of different concentrations, electrode area = 0.30 cm²

NaOH (M)	dE/dt ($mV s^{-1}$)	A_1		A_2		A_4	
		i_p (mA)	E_p (V)	i_p (mA)	E_p (V)	i_p (mA)	E_p (V)
1.00	100	0.500	−0.440	1.480	−0.050	2.00	+0.396
	50	0.300	−0.444	1.220	−0.130	1.00	+0.410
	20	0.250	−0.452	0.775	−0.195	5.50	+0.458
	10	0.150	−0.458	0.388	−0.228	9.83	+0.465
	5	0.110	−0.460	0.200	−0.241	8.25	+0.488
0.50	100	0.400	−0.410	0.600	+0.100	3.92	+0.295
	50	0.300	−0.415	0.464	0.000	1.90	+0.350
	20	0.150	−0.421	0.410	−0.125	0.68	+0.410
	10	0.100	−0.426	0.345	−0.175	0.79	+0.430
	5	*	−0.429	0.210	−0.200	1.54	+0.460
	2	*	−0.433	0.160	−0.230	1.20	+0.485
0.25	200	0.450	−0.333	0.640	*	0.000	−0.200
	100	0.260	−0.351	0.440	*	0.312	−0.100
	50	0.180	−0.371	0.700	+0.300	0.220	+0.305
	20	0.090	−0.383	1.100	+0.140	0.598	+0.375
	10	0.050	−0.395	0.950	0.000	0.449	+0.430
0.10	500	0.800	−0.250	*	*	—	—
	200	0.380	−0.300	*	*	—	—
	100	0.270	−0.326	*	*	—	—
	50	0.150	−0.341	*	*	—	—
	20	0.050	−0.353	*	*	—	—
0.05	500	0.565	−0.190	*	*	—	—
	200	0.300	−0.263	*	*	—	—
	100	0.190	−0.290	*	*	—	—
	50	0.170	−0.130	*	*	—	—
	20	0.075	−0.327	*	*	—	—
	10	0.021	−0.342	*	*	—	—

* The values cannot be determined accurately.

(in this study) with those reported previously for copper shows that: (a) peak A_1 corresponds to the formation of a Cu(OH) film [29–31]; (b) peak (or shoulder) A_2' is assumed to be due to transformation of Cu(OH) to Cu_2O [29]; (c) peak A_2 is related to the formation of a $Cu(OH)_2$ or CuO layer [29, 30, 32]; and (d) peak A_3 (shown only in highly alkaline solutions) is attributable to the oxidation of Cu(II) species to Cu(III) species [33, 34].

On the reverse scan to more cathodic potentials, another anodic peak appears (peak A_4) which is not apparent for copper. In alkaline solutions of OH^- ion concentration < 0.1 M peak A_4 did not appear. The sharpness of peak A_4 increases with decreasing scan rate. Although the peak current, $i_p(A_4)$, and the peak charge show complex dependences of both the alkali concentration and the scan rate, the peak potential $E_p(A_4)$, always shifts to more anodic values with increasing

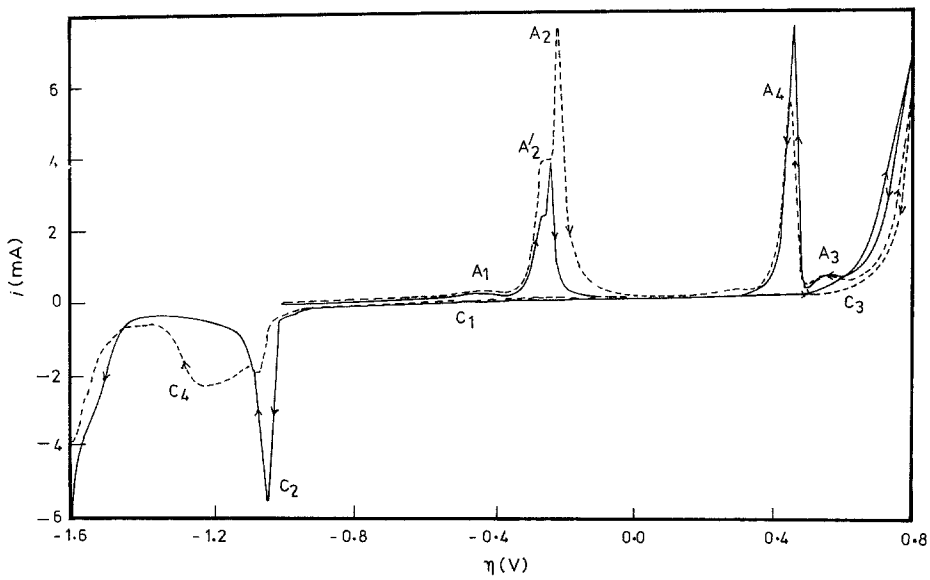

Fig. 1. Cyclic voltammograms for α-brass in 1.0 M NaOH solutions at 30° C at scan rate of (——) 10 and (– – –) 20 mV s^{-1}.

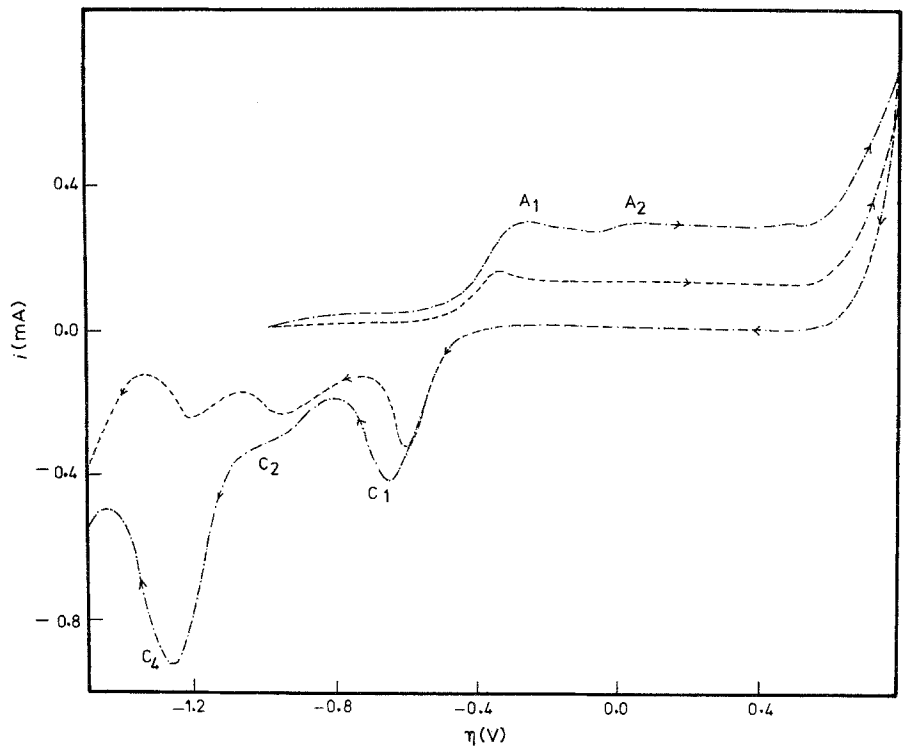

Fig. 2. Cyclic voltammograms for α-brass in 0.05 M NaOH solutions at 30° C at scan rate of (– – –) 50 and (—·—) 200 mV s^{-1}.

alkali concentration or decreasing scan rate. The anodic peak and currents are summarised in Table 1.

The cathodic peaks are interpreted as: (a) Peak C_1, corresponding to the reduction of Cu(II) species to Cu(I) [29–31]; (b) Peak C_2, including the reduction of Cu(I) species to Cu(O) [29, 32–35]; (c) Peak C_4, connected with the reduction of Zn(II) species to Zn(O); [27, 28] and (d) Peak C_3, corresponding to the reduction of Cu(III) species to Cu(II), usually observed for copper [32, 35] but which does not appear clearly in the cyclic voltammograms depicted in Figs. 1, 2.

This last peak (d) is probably due to the large contribution of the anodic current corresponding to peak A_4 which seems to mask the peak corresponding to Cu(III) → Cu(II). However, C_3 appears in other cases, as can be seen in Figs. (3–5). The cathodic peaks show complex dependence on both the alkali concentration and the scan rate, especially in solutions of $[OH^-] > 0.1$ M. Thus, in highly alkaline media, peak C_2 (Cu(I) reduction) is the most pronounced cathodic peak at low scan rate while peak C_4 (Zn(II) reduction) predominantes at higher scan rate. The contribution

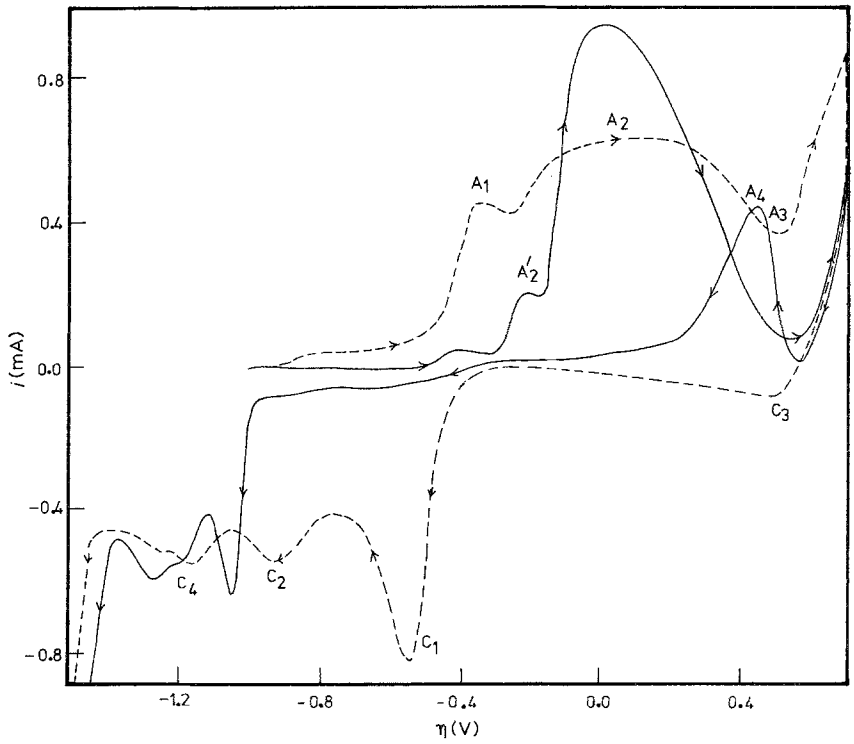

Fig. 3. Cyclic voltammograms for α-brass in 0.25 M NaOH solutions at 30° C at scan rate of (——) 20 and (– – –) 200 mV s^{-1}.

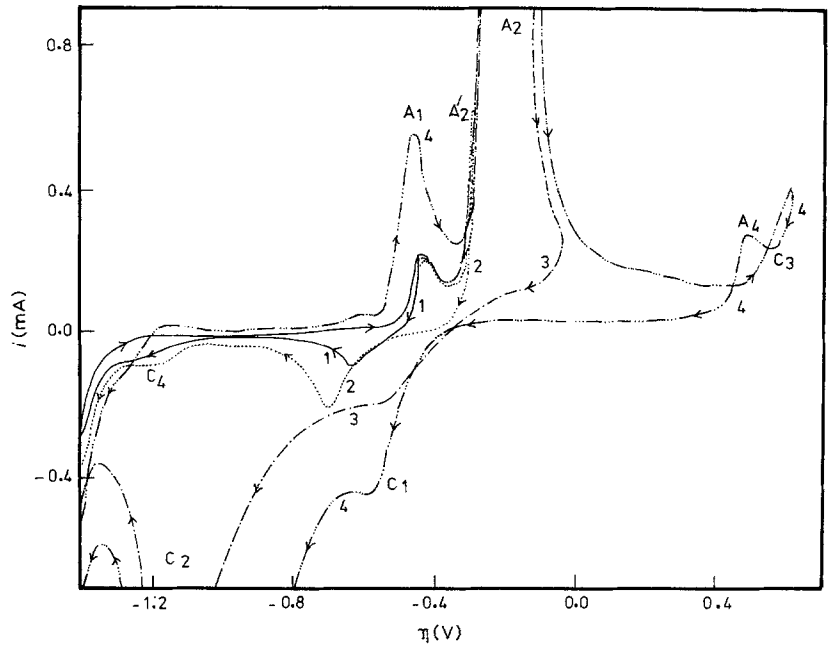

Fig. 4. Cyclic voltammograms of α-brass in 1.0 M NaOH solutions at 30° C for progressively higher positive potential in each cycle $dE/dt = 20\,mV\,s^{-1}$.

due to Cu(II) reduction (peak C_1) becomes pronounced as the alkali concentration decreases. The complex dependence of magnitude of the cathodic peaks on $[OH^-]$ and the scan rate may be explained partially in terms of the relative solubility as well as the amount of the different insoluble products formed by oxidation. In high alkali concentration, $Cu(OH)_2$ is subject to dissolution while Cu_2O is not [36, 37] and consequently the relative magnitude of peak C_1 to C_2 increases with decreasing alkali concentration. The relative amount of $Zn(OH)_2$ to that of $Cu(OH)_2$ and Cu_2O seems to be higher at high scan rate. This accounts for the predomination of peak C_4 at high scan rate, *cf.* Fig. 1.

In 0.05 M NaOH solution, the CVs in Fig. 2 show that peak C_1 is larger than peak C_2. Such findings may be explained by assuming that the reduction of Cu(I) → Cu(O) occurs partially. In fact, the electrode surface appearance after the CV experiment showed a loosely adherent anodic layer. Similar observations were observed after open-circuit corrosion in NaOH solutions and the film was found to consist mainly of Cu_2O. Thus, it may be inferred that Cu_2O is reduced partially in NaOH solutions of low concentrations ($\leqslant 0.05$). The unreduced Cu_2O is poorly attached to the surface and can be easily removed.

In 0.25 M NaOH solutions, the effect of scan rate on the cyclic voltammograms is complex (Fig. 3). At $dE/dt \geqslant 100\,mV\,s^{-1}$, the CVs are similar to that at $200\,mV\,s^{-1}$ and the dependency of i_p and E_p is similar to that observed in other cases. But at $dE/dt \leqslant 50\,mV\,s^{-1}$, peaks A_2' and A_4 become pronounced and peak A_2 is higher and sharper (CV at $20\,mV\,s^{-1}$ is an example of this). Such findings reflect the complexity

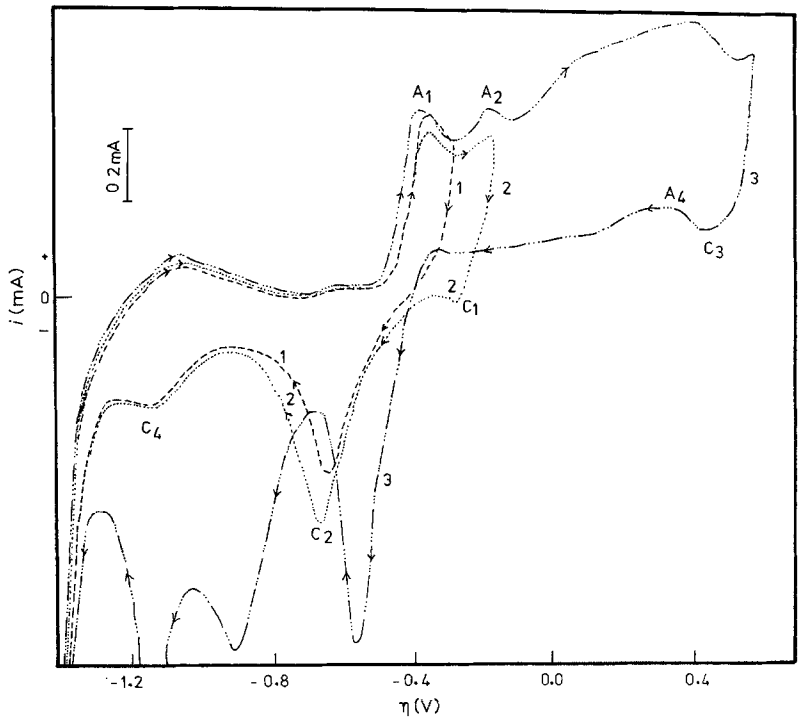

Fig. 5. Cyclic voltammograms of α-brass in 0.05 M NaOH at 30° C for progressively higher positive potential in each cycle, $dE/dt = 20\,mV\,s^{-1}$.

of the oxidation process. In fact, an abnormal effect of scan rate on the anodic peak A_2 in 0.5 M NaOH for copper was previously recorded [31]. Further, it is observed that peak C_1 in 0.25 M NaOH is larger than that in 0.05 M alkali although the formed $Cu(OH)_2$ at this peak is more soluble in the solution of higher concentration. However, investigation of the anodic parts of the corresponding CVs shows that the anodic peak in 0.25 M NaOH is larger than that in 0.05 M alkali, i.e. the amount of reducible Cu(II) formed in the former solution is higher.

The anodic and cathodic peaks can easily be seen from CVs for progressively higher potential in each cycle depicted in Figs 4, 5. The fact that peak A_2' does not represent an oxidation peak can be inferred from Fig. 5 where no additional reduction peak is shown beside that corresponding to Cu(I) reduction after the scan reverse at −1.00 V (cycle 3). The anodic and cathodic peaks at −1.3 V to −1.0 V are related to zinc in α-brass [27, 28].

In the present study the effect of scan rate on i_p and E_p for peaks A_1 and A_2 only can be quantitatively analysed. In NaOH solution $\leqslant$0.25 M, i_p and E_p corresponding to peak A_2 cannot be analysed satisfactorily due to the fusion of peaks A_1 and A_2 in a very broad and flat peak, *cf.* Fig. 2. Figs 6 and 7 show the linear dependence of both i_p and E_p for peaks A_1 and A_2 on $(dE/dt)^{1/2}$. This indicates that formation of Cu(OH) and $Cu(OH)_2$ proceeds under ohmic resistance following a dissolution-precipitation mechanism [38, 39].

Figure 8 shows the linear variation of the spontaneous redox potentials for peaks A_1 and A_2 (denoted by E' and E'') with logarithm of OH^- ion concentration. E' and E'' values were determined by extrapolation of E_p–$(dE/dt)^{1/2}$ lines to zero dE/dt values

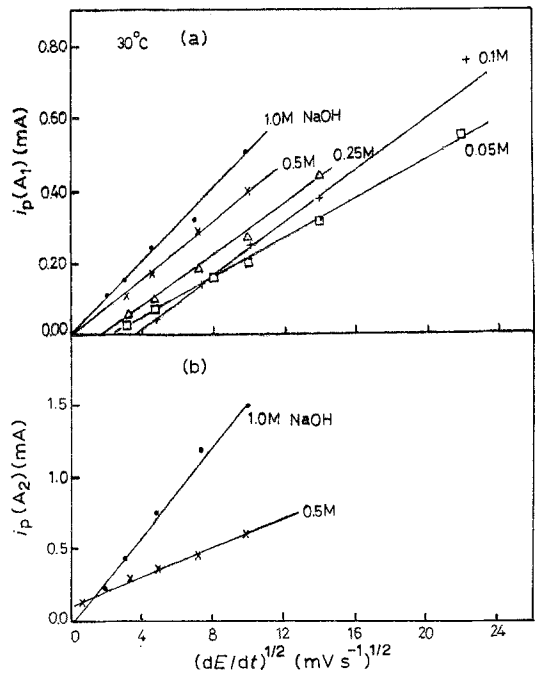

Fig. 6. Variation of the peak current, i_p, with the square root of scan rate for α-brass in NaOH solutions of different concentrations: (a) peak A_1 and (b) peak A_2.

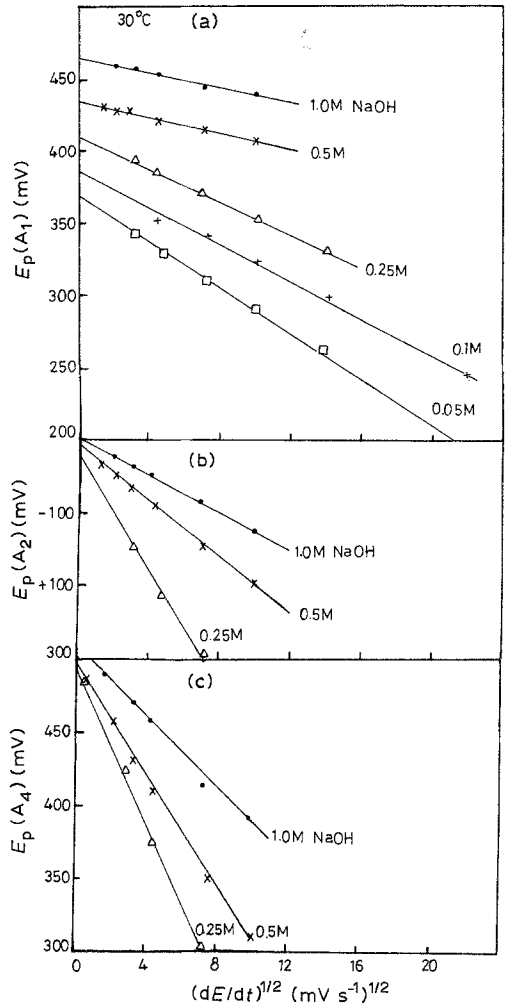

Fig. 7. Variation of the peak potential, E_p, with the square root of scan rate for α-brass in NaOH solutions of different concentrations: (a) peak A_1, (b) peakA_2 and (c) peak A_4.

[40]. The absence of a polarization effect on E' and E'' values make them most suitable for comparison with the thermodynamic data. The values of E' and E'' at log $[OH^-] = 0$, were found to be −0.458 and −0.330 V/SCE, respectively. The slopes, $dE/d \log \times [OH^-]$, for E' and E'' were 0.065 and 0.062 V decade^{-1}, respectively. At peaks A_1 the following electrode reaction is assumed:

$$2Cu + 2OH^- = Cu_2O + H_2O + 2e^- \qquad E = -0.598 - 0.060 \log [OH^-] \text{ V/SCE} \quad (1a)$$

or [29]:

$$Cu + OH^- = Cu(OH) + e^- \qquad E = -0.558 - 0.060 \log [OH^-] \text{ V/SCE} \quad (1b)$$

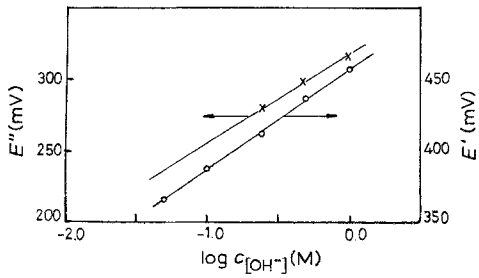

Fig. 8. Spontaneous potentials, E' and E'', against logarithm of NaOH concentration for peaks A_1 and A_2, respectively.

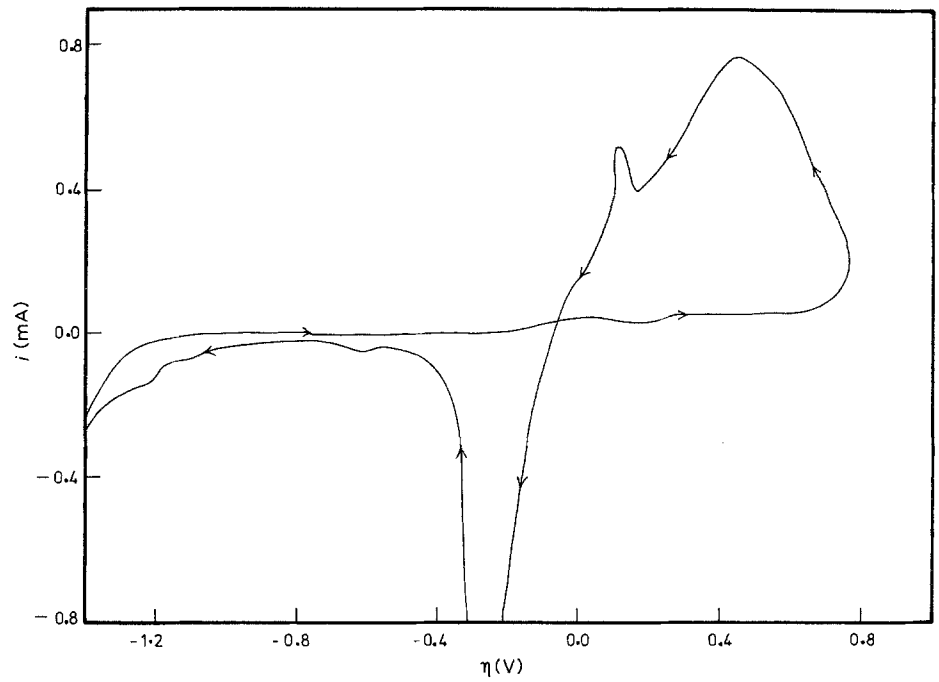

Fig. 9. Cyclic voltammograms for α-brass in borate buffer solutions of pH 9.24 at 30° C in presence of 0.2 M sodium chloride. dE/dt = 20 mV s^{-1}.

while peak A_2 is related to the reaction:

$$Cu_2O + 2OH^- = 2CuO + H_2O + 2e^- \quad (2)$$

$$E = -0.328 - 0.060 \log [OH^-] \text{ V/SCE}$$

The values E'' and $dE''/d \log [OH^-]$ are nearly coincident with those of Reaction 2, peak A_2. The E' value is more positive by 140 mV than the standard electrode potential of Reaction 1a while the slope $dE'/d \log [OH^-]$ is reasonable (5 mV decade^{-1} difference). The E' value is comparable with the peak potential corresponding to Cu_2O for copper in 1.0 M NaOH solutions [31, 35]. The shift of E' to more positive potentials may be attributed to the existence of a passive $Zn(OH)_2$ film before peak A_1. For many metals, the potential shift to more positive values is connected with the existence and development of a passive layer [41, 43].

Peak A_4 seems to be connected with peak A_3 since both appear in highly alkaline solutions only. The concentration of the soluble species Cu(III) at the electrode surface increases with increasing $[OH^-]$ and decreasing scan rate [31, 35]. At the same time, peak A_4 is higher and sharper as $[OH^-]$ increases or scan rate decreases. Thus, peak A_4 may be assumed to be due to the diffusion of Cu(III) through the passive layer to react with Zn(O) in the alloy.

The effect of halide ions (F^-, Cl^- and Br^-) on the cyclic voltammograms in 0.1 M NaOH and borate buffer solutions of pH 10.18, 9.24 and 7.26 was studied. The pitting process is absent in 0.1 M NaOH and present in the other less alkaline solutions. Fig. 9 shows the pitting process for α-brass in borate solutions of pH 9.24 in the presence of 0.2 M sodium salts of F^-, Cl^- and Br^-. The rapid increase of the current before and onset of oxygen evolution is ascribed to pitting. The current is still high even on the reverse potential scan. When the repassivation potential is attained, the current drops rapidly and becomes cathodic. The investigation of the electrode surface after the CV shows that the passive film is vigorously attacked and there are red dezincified spots. The pitting potential, E_b, was determined at dE/dt = 2 mV s^{-1}, and was found to decrease linearly with logarithm of halide ion concentration as can be seen in Fig. 10a and b. The dependence of E_b on the solution pH is irregular

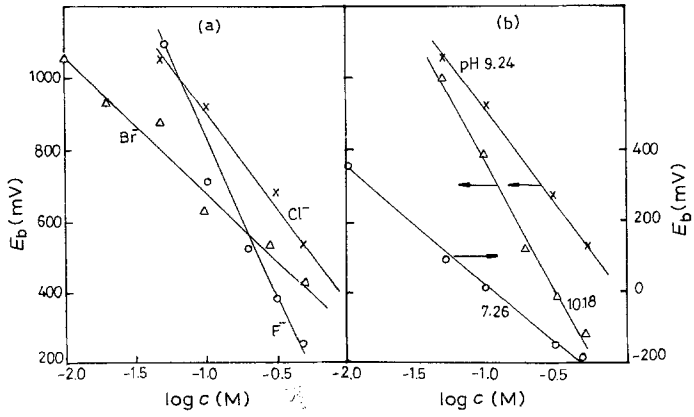

Fig. 10. (a) E_b against logarithm of halide ion concentration recorded in borate buffer solutions of pH 9.24 at 30° C: (○) F^-, (×) Cl^- and (△) Br^-, dE/dt = 2 mV s^{-1}; (b) Breakdown potential, E_b, against logarithm of chloride ion concentration recorded at 2 mV s^{-1} in borate buffer solution of pH: (○) 7.26 (×) 9.24 and (△) 10.18.

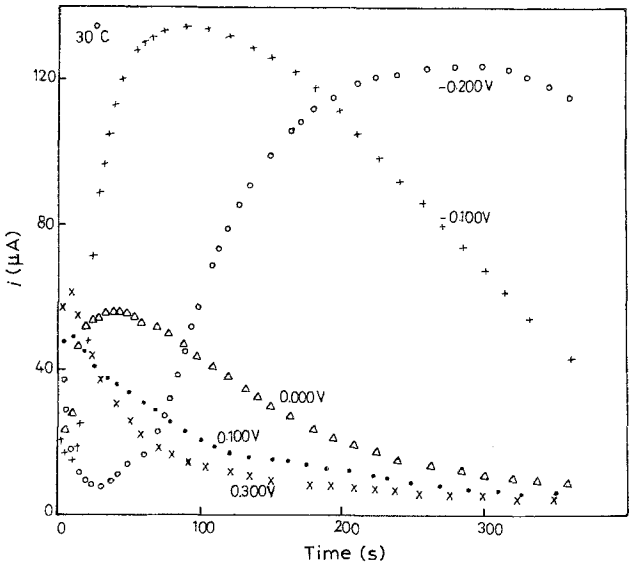

Fig. 11. Potentiostatic i–t curves for α-brass in 0.1 M NaOH at different E_s values: (○) −0.200, (+) −0.100, (△) 0.000, (●) +0.100 and (x) +0.300 V.

and depends on the halide concentration. Generally, E_b values recorded in alkaline solutions were more anodic than those recorded in neutral solutions. At $[OH^-] \geqslant 0.1$ M, the disappearance of pitting suggests the inhibitive action of OH^- ions.

3.2. *Current transients*

3.2.1. In the absence of pitting. The potentiostatic current transients for α-brass in alkaline solutions in the absence and presence of F^-, Cl^- and Br^- ions were recorded by stepping the potential at certain E_s values from steady open-circuit potentials (−0.210 to −0.305 V depending on alkali concentration). Figs 11 and 12 show some examples for E_s in the range from −0.200 to +0.300 V. The general features of the i–t curves were: the current initially decreased very rapidly, then increased to a maximum and finally, decreased slowly to a steady value at $t \to \infty$. Some i–t curves show only a gradual current decrease and no maximum or minimum can be observed. The initial current decrease is attributed to the instantaneous nucleation of a two dimensional Cu_2O film beside the already formed $Zn(OH)_2$ layer before the potential stepping at E_s [30]. The peak appearing thereafter is connected to the formation and tridimensional nucleation of $Cu(OH)_2$ or CuO [30, 44]. The current contribution due to the corrosion of the base metal under the passive layer predominates thereafter [30]. Although the quantitative analysis of i–t curves previously reported for copper is not suitable in the present work due to the complex nature of the passive layer, the general features of the i–t curves are similar to those for copper in alkaline solutions [30, 37].

The corrosion of the base metal can be regarded as a dissolution process of the three dimensional oxide nuclei proceeding under diffusion control and following a rate equation of the form [30]:

$$i = \frac{A}{(t)^{1/2}}[1 - \exp(-Bt)] \qquad (4)$$

where $A = nFD^{1/2}\Delta C/\pi^{1/2}$ and $B = K\pi DN_0$; K is the proportionality constant, ΔC is the concentration difference of Cu(II) in the layer normal to the electrode surface; D is the diffusion coefficient of the diffusing species; and N_0 is the number of available sites for corrosion. At $t \to \infty$ Equation 4 becomes

$$i = A/(t)^{1/2} \qquad (5)$$

Some examples showing the validity of Equation 5 can be seen in Fig. 13. The presence of halide ions does not substantially affect the i–t curves.

3.2.2. In the presence of pitting. In the presence of pitting, the i–t curves differ from those in the plain solutions as can be seen, for example, in Fig. 14a. Initially the current decreased very rapidly then increased rapidly to very high values. After a certain time, depending on the halide type and concentration, E_s value and the base electrolyte, the current decreased again slowly to a steady value. The part corresponding to the current rise with time (pitting corrosion current) was found to fit the Engell-Stolica Equation [45], as shown in Fig. 14b:

$$i - i_b = k(t - t_i)^b \qquad (6)$$

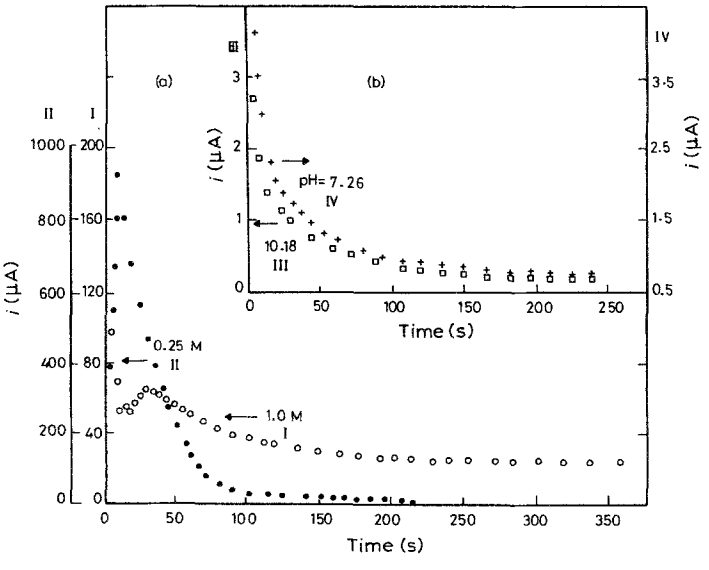

Fig. 12. i–t curves for α-brass at E_s = +0.100 V recorded in different alkaline solutions at 30°C. (a) NaOH solutions: (○) 1.00 M and (●) 0.25 M; (b) borate buffer solutions of pH: (+) 7.26 and (□) 10.18.

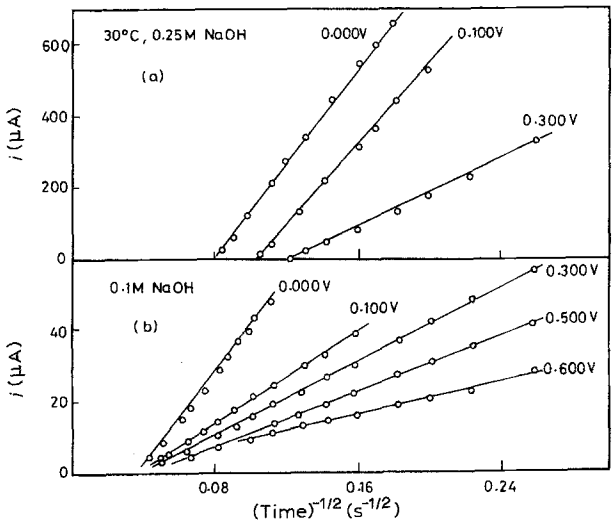

Fig. 13. Current against the reciprocal of the square root of time at different E_s values for α-brass in NaOH solutions (at 30°C) of concentration: (a) 0.25 M and (b) 0.10 M.

where i and i_b are the overall and the background apparent currents, respectively, k and b are constants and t_i is the induction time before pitting. The presence of Cl^-, Br^- or F^- ions shows the same behaviour. The pitting process can be explained as a result of the removal of the passive layer at the sites of attack which become centres for the nucleation and growth of the salt nuclei leading to the pitting corrosion [30]. The fact that the pitting is prevented in highly alkaline solution $\geqslant 0.1$ M, suggests that competitive adsorption between the corrosive ions (Cl^-, Br^-, . . .) and the inhibitor ions (OH^- ions) occurs. At low [OH^-], the adsorption of corrosive ions predominates and leads to pitting corrosion while at higher [OH^-], the adsorption of OH^- ions predominates and pitting is prevented.

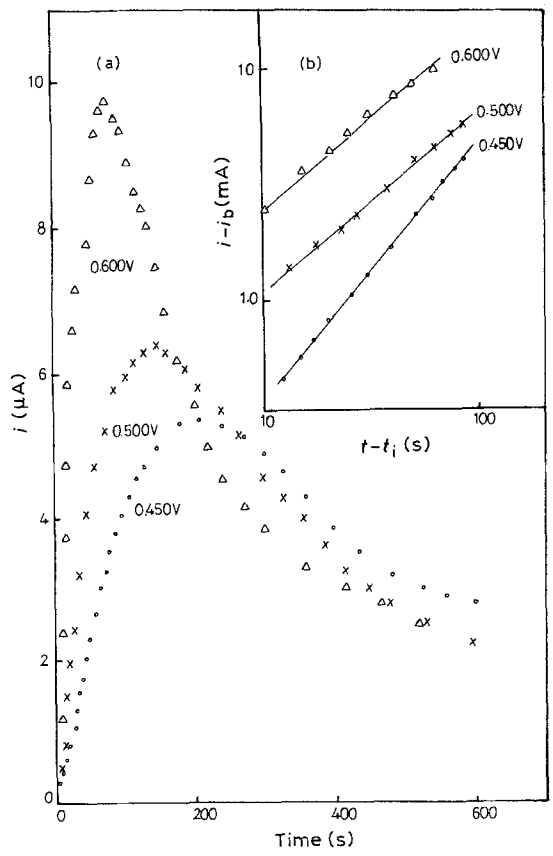

Fig. 14. (a) Current transient for α-brass in borate buffer solutions (at 30°C) of pH 9.24 in presence of 0.2 M NaCl at different E_s values: (●) 0.450, (x) 0.500 and (△) 0.600 V. (b) log ($i - i_b$) against log ($t - t_i$) relation at E_s values: (○) 0.450, (x) 0.500 and (△) 0.600 V.

References

[1] A. M. Shams El-Din and F. M. Abd El-Wahab, *Corros. Sci.* **17** (1977) 49.
[2] M. J. Müller, H. Freissler and E. Plettinger, *Z. Elektrochem.* **41** (1935) 774.
[3] H. Sugawara and H. Ebiko, *Corros. Sci.* **7** (1967) 513.
[4] H. W. Pickering and C. Wagner, *J. Electrochem. Soc.* **114** (1967) 698.
[5] H. W. Pickering and P. J. Byrne, *ibid.* **116** (1969) 1492.
[6] A. H. Taylor, *ibid.* **118** (1971) 854.
[7] V. F. Lucey, *Br. Corros. J.* **1** (1965) 9; **2** (1965) 53.
[8] E. E. Langenegger and F. P. A. Ribinson, *Corrosion* **25** (1969) 136.
[9] G. Joseph and M. T. Arce, *Corros. Sci.* **7** (1967) 597.
[10] B. Miller, *J. Electrochem. Soc.* **116** (1969) 1117.
[11] H. G. Feller, *Corros. Sci.* **8** (1968) 259.
[12] K. Balokrishnan, V. K. Venkatesan, Proceedings on the Symposium on the Chemistry and Physics of Surface Metals and their Oxides (1976) 235.
[13] H. W. Pickering, *J. Electrochem. Soc.* **117** (1970) 8.
[14] N. V. Vyazovikina, I. K. Gorkina and I. K. Marshakov, *Elektrokhimiya* **18** (1982) 1391.
[15] M. Makipaa, E. Muttilainen, T. Hakkarainen and L. Carpen, Proceedings of the 10th Scandanavian Corrosion Congress (1986) 1381.
[16] R. C. Newman, T. Shahrabi and K. Sieradzki, *Corros. Sci.* **28** (1988) 873.
[17] R. H. Heidersback and E. D. Verink, *Corrosion* **28** (1972) 397.
[18] G. M. Sparkes and J. C. Scully, *Corros. Sci.* **14** (1974) 619.
[19] R. P. M. Procter and G. N. Stevens, *ibid.* **15** (1975) 349.
[20] J. C. Scully, *Met. Sci.* **12** (1978) 290.
[21] D. J. Lees and T. P. Hoar, *ibid.* **20** (1980) 761.
[22] E. F. I. Roberts, *ibid.* **21** (1981) 177.
[23] G. T. Burstein and R. C. Newman, *Corrosion* **36** (1980) 225.
[24] L. M. Gassa and J. R. Vilche, *Corros. Sci.* **25** (1985) 245.
[25] W. A. Badawy, A. G. Gad-Allah and H. H. Rehan, *J. Appl. Electrochem.* **17** (1987) 559.
[26] A. G. Gad-Allah, W. A. Badawy, H. H. Rehan and M. M. Abou-Romia, *ibid.* **19** (1989) 928.
[27] P. F. Hutchison and J. Turner, *J. Electrochem. Soc.* **123** (1976) 183.
[28] B. Aurian-Blajeni and M. Tomkiewicz, *ibid.* **132** (1985) 1511.
[29] C. H. Pyun and S. M. Park, *ibid.* **133** (1986) 2024.
[30] M. R. G. De Chialvo, R. C. Salvarezza, D. Vasquez and A. J. Arvia, *Electrochim. Acta* **30** (1985) 1501.
[31] S. M. Abd El-Haleem and B. G. Ateya, *J. Electroanal. Chem.* **117** (1981) 309.
[32] J. Ambrose, R. G. Barradas and D. W. Shoesmith, *ibid.* **47** (1973) 47; **47** (1973) 65.
[33] A. M. Shams El-Din and F. M. Abd El-Wahab, *Electrochim. Acta* **9** (1964) 113.
[34] J. M. M. Droog, C. A. Alderliesten, P. T. Alderliesten and G. A. Bootsma, *ibid.* **111** (1980) 61.
[35] B. Miller, *J. Electrochem. Soc.* **116** (1969) 1675.
[36] D. W. Shoesmith and W. W. Lee, *Electrochim. Acta* **22** (1977) 1411.
[37] D. W. Shoesmith, T. E. Rummery, D. Owen and W. Lee, *ibid.* **22** (1977) 1403.
[38] W. J. Müller, *Trans. Faraday Soc.* **27** (1931) 737.
[39] A. J. Calandra, N. R. Detacconi, R. Pereiro and A. J. Arvia, *Electrochim. Acta* **19** (1974) 901.
[40] I. A. Ammar, S. Darwish, M. W. Khalil and S. El-Taher, *Mat-Wiss. U. Werkstofetch* **19** (1988) 271.
[41] A. K. Vijh, *Corros. Sci.* **12** (1972) 105.
[42] A. G. Gad-Allah, H. A. Abd El-Rahman and M. M. Abou-Romia, *Br. Corros. J.* **23** (1988) 181.
[43] M. M. Hefny, A. G. Gad-Allah, S. A. Salih and M. S. El-Basiouny, *Corrosion* **44** (1988) 691.
[44] B. Scharifker and G. Hill, *Electrochim. Acta* **28** (1983) 879.
[45] H. J. Engell and D. N. Stolica, *Z. Phys. Chem. Unterr.* **20** (1959) 113.